Impact of Hydrostratigraphic Continuity in Heterogeneity on Brine-to-Freshwater Interface Dynamics; Implications from a 2-D Parametric Study in an Arid and Endorheic Basin

Article *in* Water Resources Research · April 2021

DOI: 10.1029/2020WR028302

CITATIONS
5

READS
333

3 authors:

Sarah Mcknight
University of Massachusetts Amherst
8 PUBLICATIONS **22** CITATIONS
SEE PROFILE

David Boutt
University of Massachusetts Amherst
135 PUBLICATIONS **1,405** CITATIONS
SEE PROFILE

Lee Ann Munk
University of Alaska Anchorage
61 PUBLICATIONS **808** CITATIONS
SEE PROFILE

AGU ADVANCING EARTH AND SPACE SCIENCE

Water Resources Research

RESEARCH ARTICLE
10.1029/2020WR028302

Impact of Hydrostratigraphic Continuity on Brine-to-Freshwater Interface Dynamics: Implications From a Two-Dimensional Parametric Study in an Arid and Endorheic Basin

S. V. McKnight[1], **D. F. Boutt**[1], **and L. A. Munk**[2]

[1]Department of Geosciences, University of Massachusetts Amherst, Amherst, MA, USA, [2]Department of Geological Sciences, University of Alaska Anchorage, Anchorage, AK, USA

Key Points:

- Increased horizontal continuity of hydrostratigraphic units decreases the slope of brine-to-freshwater interface geometry
- Increased horizontal hydrostratigraphic continuity increases time required to reach a new dynamic steady state following change in recharge
- Density-driven flow creates variable interface geometry and sensitivity in heterogeneous media that is not captured in homogeneous media

Supporting Information:

Supporting Information may be found in the online version of this article.

Correspondence to:

S. V. McKnight,
smcknight@umass.edu

Citation:

McKnight, S. V., Boutt, D. F., & Munk, L. A. (2021). Impact of hydrostratigraphic continuity on brine-to-freshwater interface dynamics: Implications from a two-dimensional parametric study in an arid and endorheic basin. *Water Resources Research*, *57*, e2020WR028302. https://doi.org/10.1029/2020WR028302

Received 3 JUL 2020
Accepted 26 FEB 2021

Abstract Despite the prevalence of density-dependent flow systems in the brine-rich aquifers of arid climates and coastal aquifers, the impact of realistic geologic conditions on interface geometry and density-dependent time-sensitive dynamics remains poorly constrained. Salar de Atacama provides an analog for exploring interface dynamics in arid regions. A site-specific two-dimensional hydrostratigraphic interpretation is used to examine the dynamics of the brine-to-freshwater interface. With the same simulation framework and core data, a separate parametric series of hydraulic conductivity distributions with varying horizontal continuity provides a mechanistic explanation for observed dynamics. Comparing modeled interfaces and their sensitivity to perturbations in recharge in each realization yields insight into interface dynamics coupled with horizontal continuity in subsurface heterogeneity. Recharge fluctuation is introduced to each distribution following the interface reaching a dynamic steady state. Metrics for results evaluation include interface slope geometry, interface width, migration length, and response rate. Analyses suggest that the average slope of the modeled interface shallows by 0.01 and 0.05 $m \cdot m^{-1}$ for an increase in continuity of highly permeable pathways by a factor of two and three, respectively. Increasing continuity also increases the overall response times and the variability in response. Results indicate that accurate representations of transient dynamics in modeling density-dependent brine-to-freshwater interface dynamics requires the consideration of heterogeneity, as saline intrusion in the highest continuity group extends over twice as far on average and the modeled interface takes over 43% more time on average to reach a new dynamic steady state when compared to their homogeneous counterparts.

Plain Language Summary Differences in the density of groundwater from dissolved salt causes groundwater flow to behave differently under different subsurface conditions. This paper focuses on how spatial differences in porosity affects flow behavior and changes the risk of saline groundwater intrusion. Core and groundwater data from the southeastern edge of the salt flat in Salar de Atacama provides information on subsurface physical characteristics and groundwater chemistry. This data is used to create an interpretation of how flow properties vary in time and space. This provides a means for assessing the impact of spatially variable geology on the geometry and the sensitivity of the brine-to-freshwater interface to changes in recharge to an aquifer. We use distributions of the area's geology to test different amounts of geologic variability in the horizontal versus the vertical direction. Results indicate that more horizontal continuity shallows the geometry and increases the time required for a brine-to-freshwater interface to reach a new position following a change in recharge. These model results suggest that it is important to consider how differences in the flow properties of different geologic units impact the response time and the extent of saline intrusion in deserts as well as any other areas that might have salty groundwater.

1. Introduction

Numerical simulations of density-dependent flow assess the risk of saline groundwater intrusion in coastal areas (Heiss & Michael, 2014; Meng et al., 2002; Trabelsi et al., 2013), and in arid and often endorheic basins where evaporation outpaces recharge and concentrates solutes in groundwater (Stein et al., 2019). The discrepancy in fluid density develops an interface where the denser brine underlies the less dense fluid to create a freshwater lens, which is commonly known as a brine-to-freshwater interface (Duffy & Hassan, 1988;

Fan et al., 1996; Houston et al., 2011; Philip & van Duijn, 1996; Wooding et al., 1997). For interfaces located in arid and endorheic basins, the processes that control the geometry and sensitivity of such interfaces remain unconstrained (Tejeda et al., 2003; Vásquez et al., 2013). The global decline of groundwater storage in aquifers in endorheic basins (Wang et al., 2018) increases the need to refine density-dependent dynamics when coupled with perturbations in recharge in such environments (Condon & Maxwell, 2019).

The Ghyben-Herzberg approximation (Morgan et al., 2012) serves as a simple analytical solution to approximate the geometry of the brine-to-freshwater interface (Post et al., 2018), but it cannot account for time-dependent dynamics of density-dependent flow. Numerical simulations represent a tool for time-dependent analysis of saline intrusion, but simulations of saturated subsurface density-dependent fluid flow in homogeneous porous media do not ubiquitously capture the interface's geometry under realistic hydraulic conditions due to influences from heterogeneity (Post et al., 2007). Density-dependent numerical simulations of brine-to-freshwater interfaces in arid basins have either been homogeneous (Tejeda et al., 2003; Vásquez et al., 2013) or simply layered models of local geology that underestimate basin-scale heterogeneity and produce unrealistic results of the modeled interface (Marazuela et al., 2018). Previous geostatistical modeling documented the influence of subsurface heterogeneity on seawater circulation in coastal aquifers (Geng et al., 2020; Kreyns et al., 2020; Michael et al., 2016). However, the extent to which the continuity of subsurface heterogeneity impacts time-sensitive dynamics in general and the interface geometry for aquifers in arid basins specifically remains unconstrained.

This paper documents that heterogeneity influences both the steady-state geometry of the brine-to-freshwater interface and the time-sensitive reaction of the interface in response to perturbations in recharge. Salar de Atacama (SdA) provides an ideal site for assessing the role of heterogeneity because of its complex structural history (Reutter et al., 2006) and extensive development of evaporite sequences (Jordan et al., 2004). Field observations document that the interface between the brine and freshwater along the southeastern margin of SdA has a shallow geometry that has not yet been captured by previous density-driven flow simulations the basin (Figure 1). As shown in Figure 1, other published observed interfaces at SdA indicate similarly shallow geometry. Yet previous literature has neither presented density-driven flow simulations that express such shallow geometry nor presented a mechanistic framework to explain the hydrogeologic dynamics that would result in such interface expressions. A geostatistical approach with equally probable distributions of hydraulic conductivity based on field data from SdA provides a means for investigating the role of continuity in heterogeneous geology on density-driven dynamics. This represents the first attempt to constrain the impact of subsurface heterogeneity on brine-to-freshwater interface geometry for arid and endorheic basins specifically. Our findings are also the first definition of time-sensitive response of saline intrusion to perturbations in recharge in relation to variations in continuity.

2. Background

2.1. Hydrogeologic Setting of Salars

Salars ("salt flats") comprise brine-bearing aquifers with subsurface heterogeneity in porous media and distinct hydrologic dynamics. Salars primarily consist of evaporites in basins with an annually negative hydrologic budget on average (Rosen, 1994; Hernández-López et al., 2014; Tyler et al., 2006). Endorheic basins provide an ideal environment for evaporite accumulation due to their tendency to inhibit the effective discharge of incoming sources (Eugster, 1980; Houston et al., 2011), but salars also occur in open basins with a negative water budget (Rosen, 1994). Brine that is more saline than seawater (>35 ppt) can occur, and the higher discrepancy in density results in a relatively shallower slope in the interface between the brine and freshwater (Yechieli, 2000). Figure 2 illustrates how salars can develop a range of stratigraphically complex aquifers, and how density-driven freshwater upwelling occurs above the brine-to-freshwater interface in brine-bearing aquifers. Their climate-sensitive change in areal extent can create a series of interbedded lithologies (Houston, 2009), and this interbedding at SdA is specifically documented in Munk et al. (2020). Since brine-bearing aquifers commonly exist in tectonically active endorheic basins (Yager et al., 2017), faulting among lithologies further complicate the lateral continuity of subsurface heterogeneity and produce interface geometries that defy theory when intersecting fault systems (Yechieli, 2000). This study therefore provides a sensitivity analysis for investigating the role of heterogeneity in density-dependent dynamics of such aquifers.

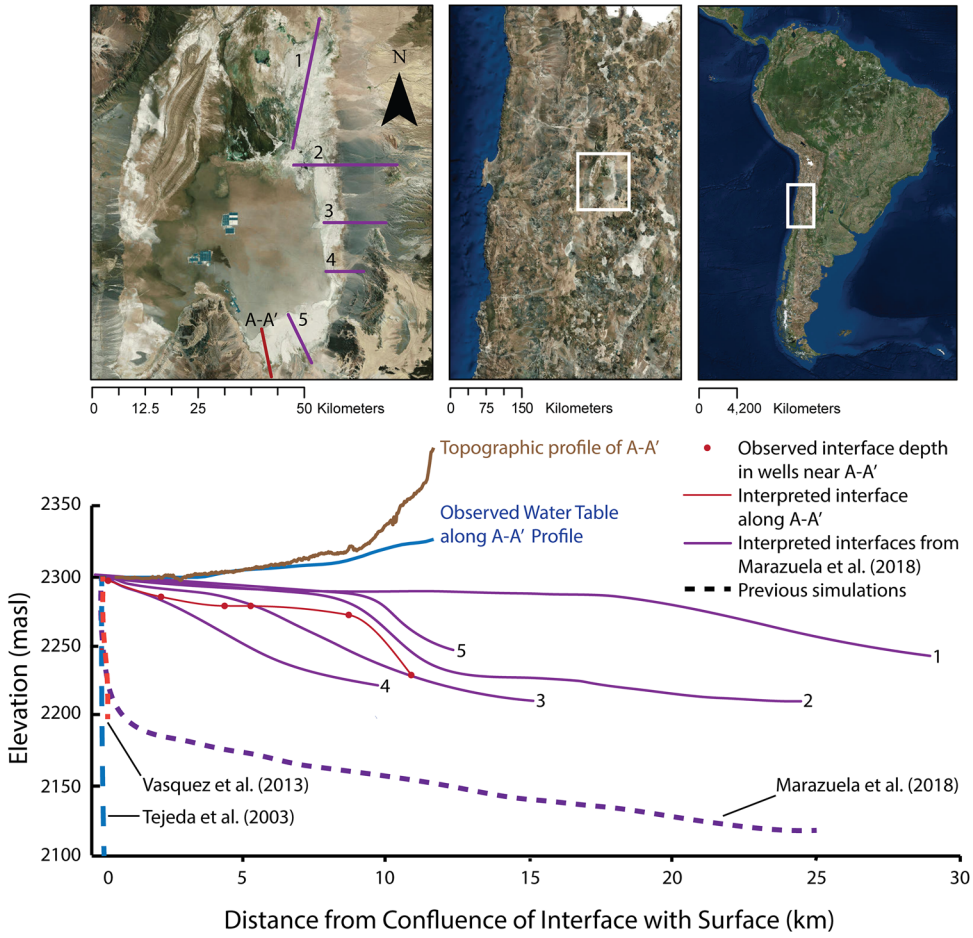

Figure 1. Comparison of observed two-dimensional (2-D) brine-to-freshwater interface locations (solid lines) with numerical simulations from previous literature (dashed lines) of the interface along the transitions zone of Salar de Atacama. Interfaces 1–5 (purple solid lines) correspond with A-E from Marazuela et al. (2018). The observed interface (red points) with interpolated geometry (red line) for this study is denoted as the A-A′ transect and its location is also shown on the reference map. The topography (brown line) and water table (blue line) for A-A′ is also included in the 2D cross section.

Aquifers in these environments also exhibit recharge-controlled water table configurations (Haitjema & Mitchell-Bruker, 2005). The resulting lateral inflow dominates long-term recharge as predicted by the Toth flow model (Carmona et al., 2000; Qureshi, 2011; Rissman et al., 2015), which can include groundwater flow into a topographically separate and relatively upgradient basin (Maxey, 1968; Montgomery et al., 2003; Schaller & Fan, 2009). Therefore, while surface recharge provides a mechanism for sustaining groundwater levels (Boutt et al., 2016) and solute delivery (Munk et al., 2018), lateral subsurface inflow represents the long-term recharge mechanism (Houston, 2009; Scanlon et al., 2006; Ye et al., 2016). Basin-scale recharge trends in arid climates can change over relatively short (i.e., interdecadal and millennial) timescales (Placzek et al., 2009), highlighting the importance of considering climate-driven shifts even if short-term hydrology appears to be stable (Zhu et al., 1998). To date, there has been no study that has characterized the impact of heterogeneity on the time-sensitive response of brine-to-freshwater interfaces to perturbations in subsurface lateral inflow (Ferguson & Gleeson, 2012; Sanford & Pope, 2010). The framework for the numerical simulations include subsurface lateral inflow as the main source of recharge and evaporation at the margin of the modeled salar as the primary source of discharge.

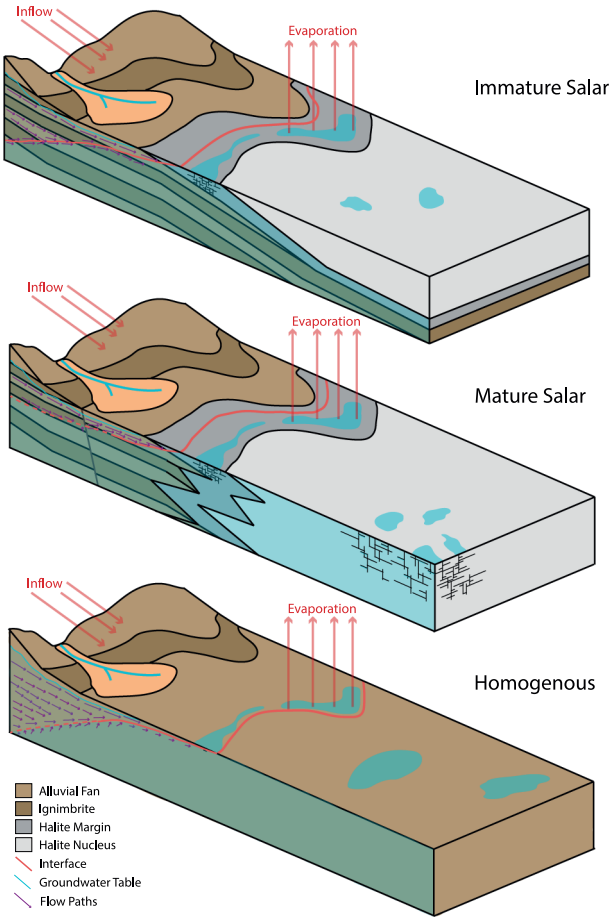

Figure 2. Conceptual illustration of mature versus immature salars and their homogeneous counterpart, with the resulting brine-to-freshwater interface and flow vectors of inflowing freshwater recharging the aquifer. Adapted from Houston et al. (2011).

2.2. Sensitivity Analyses on Density-Driven Flow Systems

Many studies have documented and simulated density-dependent flow and its resulting brine-to-freshwater interface in both coastal (Trabelsi et al., 2013; Werner & Simmons, 2009; Yechieli, 2000) and inland aquifers (Fan et al., 1996; Tejeda et al., 2003; Wooding et al., 1997). Studies that numerically assess the factors that impact saline intrusion commonly examine a single influence on the interface's dynamics, such as changes in recharge (Post et al., 2019) or discharge (Werner & Simmons, 2009). For coastal aquifers, studies primarily focus on coupling density-dependent flow with solute transport in order to define the risk of saline groundwater intrusion to inland groundwater resources (Meng et al., 2002; Morgan et al., 2012; Werner & Simmons, 2009). Such studies frequently investigate the sensitivity of brine-to-freshwater interface migration via solute transport coupled with various influences, including but not limited to the buoyancy effect from density-dependent flow (Bear, 1972; Werner et al., 2013), wave-induced groundwater circulation cells (Heiss et al., 2017), fluctuating circulation from tidal forcing (Bailey, 2015; Heiss & Michael, 2014), variations in circulation cell size from bedform topography (Konikow et al., 2013), increased landward interface migration from sea level rise (Ketabchi et al., 2016; Yechieli et al., 2010), increased supratidal salinity from evaporation (Geng & Boufadel, 2015), increased interface migration via preferential pathways from conducive faulting (Trabelsi et al., 2013), anthropogenic pumping of inland fresh groundwater (Ferguson & Gleeson, 2012), different upscaling techniques (Held et al., 2005), and heterogeneity in geologic media (Heiss et al., 2020; Kerrou & Renard, 2010; Liu et al., 2014; Mahmoodzadeh & Karamouz, 2019; Michael & Khan, 2016; Michael et al., 2016; Pool et al., 2015). While studies of saline groundwater intrusion primarily focus on coastal environments, inland and arid basins are also prevalent sites of brine development (Rissman et al., 2015). Arid basins further comprise evaporite-dominated geology and arid geomorphology that is unique from coastal environments and yet remains uncomprehensively modeled on a global scale (Houston et al., 2011).

2.3. Numerical Simulations of Density-Dependent Flow & Heterogeneity

Since geologically heterogeneous media comprise the majority of aquifers (Gelhar et al., 1992), many numerical studies have investigated the impact of subsurface heterogeneity on density-dependent flow dynamics in order to elucidate more realistic mechanistic explanations for the documented salinity distributions and transport flowpaths (Schincariol et al., 1997). Heiss et al. (2020) establish that hydraulically conductive stratigraphic features can control spatial variations in geochemical fluxes that have been observed and documented in previous studies (Russoniello et al., 2013; Sawyer et al., 2014). Michael et al. (2016) provide an extensive analysis on the impact of geologic heterogeneity on seawater circulation, while Kreyns et al. (2020) document that freshwater discharge can extend further offshore in heterogeneous volcanic aquifers when compared to homogeneous counterparts. Geng et al. (2020) use simulations to investigate the impact of subsurface heterogeneity on tidally influenced circulation, thereby confirming the importance of coupling heterogeneity with influences on an aquifer's hydrologic dynamics in order to further constrain geologic impacts on solute transport. Michael and Khan (2016) further detail heterogeneity's influence on variable solute transport and decreased travel time through an aquifer in response to relatively deeper groundwater pumping. Klammler et al. (2020) document that freshwater aquifer storage in coastal aquifers may experience a multi-decadal time lag in response due to changes in recharge resulting from fluctuations in brine-to-freshwater interface migration. Yet the impact of continuity in heterogeneity on further increasing such a time lag remains unconstrained. This study therefore aims to further define how continuity in

basin-scale heterogeneity impacts the time sensitivity of density-dependent response to perturbations in recharge.

Given the resource-rich importance (Kunasz, 1980; Munk et al., 2016) and prevalence of brine-bearing aquifers underlying inland and arid basins (Yechieli & Wood, 2002; Wang et al., 2018), simulating density-dependent flow in these systems has increased in recent years. Evapoconcentration in these basins provide a mechanism for elevated concentrations of lithium in groundwater, and as a mining resource, these groundwater reserves represent approximately three-fourths of global lithium production (Kesler et al., 2012; Munk et al., 2016; Steinmetz, 2017). These basins' unique hydrologic conditions, such as lack of tidal influence and distinct evaporation patterns (Hernández-López et al., 2014), further elevate the need for environment-specific modeling. Simulations of density-dependent dynamics in arid, inland basins commonly model either homogeneous conditions (Tejeda et al., 2003) or simple stratigraphic interpretations with continuous, single-layer aquitards (Duffy & Hassan, 1988; Marazuela et al., 2018). While Marazuela et al. (2018), document the shallowing of the interface which presumably results from an underlying hydraulically confining unit, the resulting modeled interface does not capture realistic geometry (Figure 1). While continuity in stratigraphic units' hydraulic conductivity increases saline groundwater circulation (Michael & Khan, 2016), the degree to which basin-scale hydrostratigraphic complexity influences salinity distributions and thus brine-to-freshwater interface geometry remains unclear for arid basins (Houston et al., 2011). The series of numerical simulations presented here represent the first attempt to characterize the impact of heterogeneity on brine-to-freshwater interface geometry for arid and inland basins specifically, as well as provide insight on the impact of heterogeneity on density-dependent dynamics to changes in recharge for brine-bearing aquifers in general. This work's importance stems from the need to understand the interplay between freshwater and brine in these basins as pressures continue to mount on freshwater and resource extraction.

3. Simulations

Saturated density-dependent groundwater flow was simulated using SEAWAT, a cell-centered finite difference approximation that solves both saturated fluid flow and solute transport (Langevin & Guo, 2006). We investigate the role of heterogeneity by varying distributions of hydraulic conductivity with a geostatistical approach. To address the site-specific implications for SdA, a separate hydrostratigraphic framework (HSF) was developed for the A-A′ transect shown in Figure 1, where brine underlying the salar interacts with shallow subsurface laterally inflowing freshwater to create a brine-to-freshwater interface along the southeastern margin (Figure S3). The HSF relies on a geologic model that was developed from core and well data, geophysical surveys, and knowledge of surface geology and basin structure based on previous literature (Jordan et al., 2002; Lowenstein et al., 2003; Mpodozis et al., 2005; Reutter et al., 2006), as further described in the Section S1.

3.1. Boundary & Initial Conditions

The structure of the finite difference grid and boundary conditions for all simulations are based on representations of aquifer characteristics for the modeled basin, including recharge via subsurface lateral inflow, discharge via evaporation, and topography based on the A-A′ transect (Figure 1). Initial conditions were calibrated during the sensitivity analyses conducted for the HSF. Excepting changes in recharge and the hydraulic conductivity distributions, all other physical boundary and initial conditions remain constant. Figure 3 illustrates the initial and boundary conditions used in all simulations for this study. The simulated domain is 13,000 m long by 300 m deep and is discretized into 100 m long by 10 m deep grid cells. The framework represents one side of a basin because the hypothetical symmetry of a basin renders the simulation of both sides redundant and therefore unnecessary. The surface boundary is based on smoothed elevation models of the topography at SdA from the available 10 m-resolution digital elevation data. A Dirichlet boundary represents specified head for the modeled edge of the nucleus, which is set to 1 m below the modeled nucleus surface, which is located in the upper left area of Figure 3. The entire left side of the model domain that represents the edge of the nucleus has a constant dissolved salt concentration of 0.2 g cm^{-3} which represents the maximum concentration observed in highly saline brines. This condition assumes that halite-dominant geology that is common in mature salars would represent a constant salinity source, as

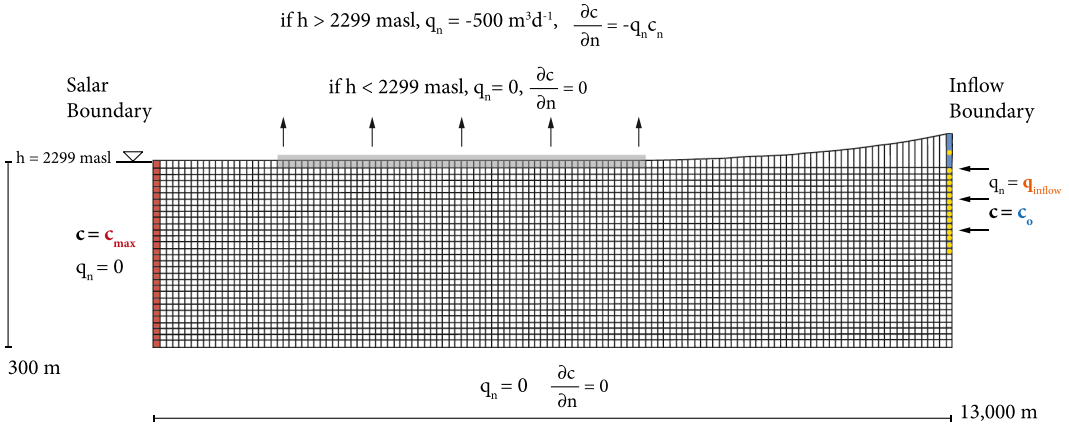

Figure 3. Boundary conditions for the 300 m deep by 13,000 m long two-dimensional model framework. Note that the model is discretized into 30 by 130 cells, and each cell has the dimensions of 10 m deep by 100 m wide. Also note that $c_{max} = 0.2$ g·cm^{-3}, $c_o = 0$ g·cm^{-3}, and that q_{inflow} varies by 300, 500, and 700 m^3·d^{-1}. Vertical exaggeration is 10.

interacting fluid would reach saturation with respect to halite. A Neumann boundary condition represents the simulated subsurface recharge of freshwater in the upper right side of the model domain as seen in the upper right area of Figure 3; this boundary condition has no concentration of dissolved salt ($c_o = 0$ g cm^{-3}). Simulated discharge via evaporation is represented as a Neumann boundary that is equivalent to the baseline inflow flux of 500 m^{-3} d^{-1}; it is a head-dependent flux that functions if simulated freshwater equivalent head is either at or less than 1 m from the modeled surface (Figure 3). Evapoconcentration was not included as a source of salinity. All other boundaries not otherwise described have no flux of either fluid or solute. The initial solute concentration for the entire extent of the domain is 0 g·cm^{-3}. Initial head values are 1 m below the modeled surface. Values of longitudinal, horizontal transverse, and vertical transverse dispersivity in all models are 10, 1, and 0.01 m respectively. These values are consistent with modeling aquifers of this scale (Gelhar et al., 1992). All iterations run with the above-described initial conditions to 3·10^6 days. The models then run for another 3·10^6 days following a perturbation in hydrologic conditions in order to assess the sensitivity of the brine-to-freshwater interface. Table 1 lists relevant parameters for the numerical simulations.

Table 1
Parameters for the Numerical Modeling Approach

Parameter	Value	Unit
Domain length	13,000	m
Domain thickness (b)	300	m
Longitudinal dispersivity (α_L)	10	m
Horizontal transverse dispersivity (α_H)	1	m
Vertical transverse dispersivity (α_V)	0.01	m
Diffusion coefficient	1·10^{-9}	m^2·s^{-1}
Effective porosity (ϑ)	0.3	–
Constant head at nucleus boundary	2,299	masl
Freshwater density (ρ_o)	1	g·cm^{-3}
Brine density (ρ_{max})	1.2	g·cm^{-3}
Storativity (S_s)	1·10^{-4}	m^{-1}
Specific yield (S_y)	0.02	–
Vertical anisotropy (Kh/Kv)	10	–

Note. These conditions are constant throughout the every simulation. Note that the listed vertical anisotropy value applies for the non-isotropic models.

3.2. Simulating Perturbations in Recharge

Groundwater inflow is the only boundary condition in this study that experiences variation for every realization of hydraulic conductivity. The simulations were run to an initial dynamic steady state which is defined as no definitive movement of the interface's position in order to establish an interface geometry from initial conditions. Each realization is subsequently exposed to two different recharge scenarios as step functions: an increase in recharge of 200 m^3·d^{-1} (i.e. total of 700 m^3·d^{-1}) and an equal decrease in recharge (i.e. a total of 300 m^3·d^{-1}). The development of the boundary condition representing recharge is based on the assumption that arid hydrology relies on interbasin flow that is characterized by long residence times and therefore prolonged variations in recharge, as supported by site-specific data (Corenthal et al., 2016; Houston, 2009; Ortiz et al., 2014). While previous numerical studies have included direct recharge (Marazuela et al., 2018), the impact of direct recharge from precipitation is not considered in this study because arid basins recharge 0.1%–5% of precipitation (Scanlon et al., 2006) and the dominant recharge mechanism of such basins is lateral groundwater flow following the Toth model (Schaller & Fan, 2009). Each simulation was run to 3·10^6 days both prior and subsequent to the simulated perturbation in recharge.

3.3. Distributions of Hydraulic Conductivity

To address the role of heterogeneity on brine-to-freshwater interface sensitivity, we use a geostatistical approach with a series of realizations of hydraulic conductivity fields by kriging available hydrogeologic data for SdA with a Markov approach using T-PROGS (Carle, 1999). We base the transition probabilities for the distributions of hydraulic conductivity on the lithologies documented from diamond drill cores recovered from the southeastern margin of SdA (S1). Realizations of heterogeneous distributions were based on hydraulic conductivity values assigned to lithostratigraphic units from the study site in the southeastern margin of SdA. Hydraulic conductivity values are based on correlating geologic and hydraulic data from the 26 cores (Table S1) and 43 wells (Table S2) from within the ~130 km^2 area that comprises the southeastern margin of SdA. The hydrostratigraphic correlation is based on over 50 hydraulic tests that have occurred in the area. Hydrostratigraphic interpretations were separated into five lithologic facies with assigned hydraulic conductivity based on the conceptualization in Munk et al. (2020): medium-grain clastic from alluvial fan deposits (10 $m{\cdot}d^{-1}$), fine-grain carbonate (1 $m{\cdot}d^{-1}$), vuggy carbonate (100 $m{\cdot}d^{-1}$), un-fractured ignimbrite (0.01 $m{\cdot}d^{-1}$), and interbedded gypsum and carbonate (0.1 $m{\cdot}d^{-1}$). Hydraulic conductivity values were determined within one standard deviation from the average for each lithostratigraphic facies. For all realizations, the proportions for fine carbonate, alluvial fan deposits, ignimbrite, vuggy carbonate, and interbedded gypsum and carbonate were 43%, 24%, 19%, 8%, and 6%, respectively.

Three groups of realizations with distinct horizontal to vertical stratigraphic continuity ratios (c_h/c_v) were created to address the role of geologic complexity in the geometry and time sensitivity of interface response: Equal continuity in both directions ($c_h/c_v = 1$), increased horizontal continuity by a factor of two ($c_h/c_v = 2$), and increased horizontal continuity by a factor of three ($c_h/c_v = 3$). For each group, the length of transition probabilities for lithologic units in the horizontal direction were multiplied by their respective c_h/c_v factor. Thirty-seven realizations of hydraulic conductivity were created for each group. The effective conductivity (K_{eff}) values for the realizations range within 5.3 $m{\cdot}d^{-1}$ and 20.3 $m{\cdot}d^{-1}$, according to Darcy flux estimates. While these realizations are based on the same hydraulic data as the HSF, they differ in that they are randomized distributions that only share the same hydraulic conductivity values with the HSF at the observation points that informed their development.

3.4. Metrics for Assessing Interface Geometry & Response to Recharge Variations

For each simulation, velocity fields, solute concentration, and resulting freshwater equivalent head values were collected. Four metrics were used to assess the simulation results for differences in interface geometry and response to perturbations in recharge. The first metric is the average slope of the interface, which was assessed with a linear best fit for each simulated interface after reaching an initial steady state. Second, another metric for assessing the physical expression of the interface is the horizontal width of the interface transition zone, which is defined as the simulated salinity concentrations that range between brackish (i.e. <0.04 $g{\cdot}cm^{-3}$) and highly saline (i.e. >0.18 $g{\cdot}cm^{-3}$) groundwater (L). Third, the length of the interface's maximum migration in the horizontal direction (L) provides an assessment of the spatial sensitivity of interface migration following a change in recharge to the modeled aquifer. Fourth, the time-sensitivity of the interface's response following a perturbation in recharge can be characterized as proportional to an exponential rate as defined by:

$$\frac{[m]_{\text{f}}}{[m]_{\text{i}}} = e^{-\text{kt}} \tag{1}$$

where $[m]_f$ is the final simulated mass of salt following a perturbation, $[m]_i$ is the initial mass prior to the perturbation, and k is the rate of change in the mass (i.e., "e-folding time"). Solving for k results in the following:

$$k = \frac{log\left(\frac{[m]_{\text{i}}}{[m]_{\text{f}}}\right)}{t} \tag{2}$$

For this study, time constant k represents the rate of change in the total mass of modeled salt in the domain, assuming that mass is conservative. Further assuming that interface movement is proportional to the total mass of salt in the simulation, the e-folding time therefore indicates the interface's relative response rate, with the amount of time corresponding to the relative rate of interface response to a perturbation in recharge. This metric represents one of several ways to assess interface stability, such as interface toe movement (Morgan et al., 2012).

We additionally assess flow topology using the Okubo-Weiss (OW) method in order to facilitate a mechanistic explanation for the relationship between the spatial characterization of the flow field and the observed physical characteristics expressed in the simulation results (Okubo, 1970; Weiss & Provenzale, 2008). The OW parameter is defined as:

$$OW = \left(\frac{\partial v_x}{\partial x} - \frac{\partial v_z}{\partial z}\right)^2 + \left(\frac{\partial v_z}{\partial x} + \frac{\partial v_x}{\partial z}\right)^2 - \left(\frac{\partial v_z}{\partial x} - \frac{\partial v_x}{\partial z}\right)^2 \quad (3)$$

where v_x and v_z represent the flow velocity in the x (i.e. horizontal) and z (vertical) directions (Geng et al., 2020). Flow topology can be characterized as either vorticity-dominated flow ($OW < -0.2\sigma_{OW}$) which indicates relatively more vertical flow and a higher likelihood for advection, or strain-dominated flow ($OW > 0.2\sigma_{OW}$) which indicates relatively high horizontal flow and more lateral dispersive solute mixing. Geng et al. (2020) and de Barros et al. (2012) provide further explanation of the OW parameter.

4. Results

4.1. Geometry & Dynamic Response of the Hydrostratigraphic Framework of Salar de Atacama

Figure 4 shows the solute concentration values, flow velocity fields, and the resulting freshwater equivalent head field of both the HSF of SdA and the homogeneous model that represents the K_{eff} of the HSF. For the homogeneous results, solute concentration values show a consistent transition zone width from 0 to 0.2 g·cm^{-3} with depth, though the upper 50 m of the model near the area of modeled evaporation increases in transition zone width. The flow velocity fields for both simulations coincide with the geometry of concentration values to represent freshwater upwelling, with higher velocity values concentrated both at and above the simulated interface between brine and freshwater. Yet the two simulations diverge in the physical distribution of concentration and velocity.

Compared to its homogeneous counterpart, concentration results from the heterogeneous model that represents the HSF of SdA indicate a shallower interface that conforms with observed concentration values within 10 m at depth. Simulated concentration results shown in Figure 4 also indicate a varying width of the brine-to-freshwater transition zone from sharp (<100 m) to diffuse (>100 m). The flow velocity field similarly expresses sharp to gradual transitions from high to lower values. The majority of the high flow velocity is concentrated in the upper surficial layer of the domain and coincides with the laterally subsurface inflowing recharge. The response time to inflow perturbations is larger by at least a factor of three for the HSF model when compared to the homogeneous model (Table S3). The total distance that the interface travels as a result of a change in inflow, as assessed through the movement of the 0.5 isoconcentration line, likewise exhibits a distinct difference between the heterogeneous and homogeneous models, with increased interface travel through permeable pathways within the heterogeneous model (Table S3).

4.2. Geometry & Dynamic Response of the Geostatistical Realizations of Hydraulic Conductivity to Changes in Inflow

Simulations with equally probable hydraulic conductivity distributions produce time-sensitive physical results that diverge from their homogeneous counterparts and show a statistically significant relationship with stratigraphic continuity in a geologically complex environment (Table S4). Figure 5 provides an example of these results from each group of realizations, including the hydraulic conductivity distribution, salt concentration distribution, freshwater equivalent head distribution, and flow velocity fields. Figure 6 shows the interface geometry results for each simulation of the hydraulic conductivity realization, which were statistically significant when separated by c_h/c_v and decreased in slope as c_h/c_v increases. The average slope

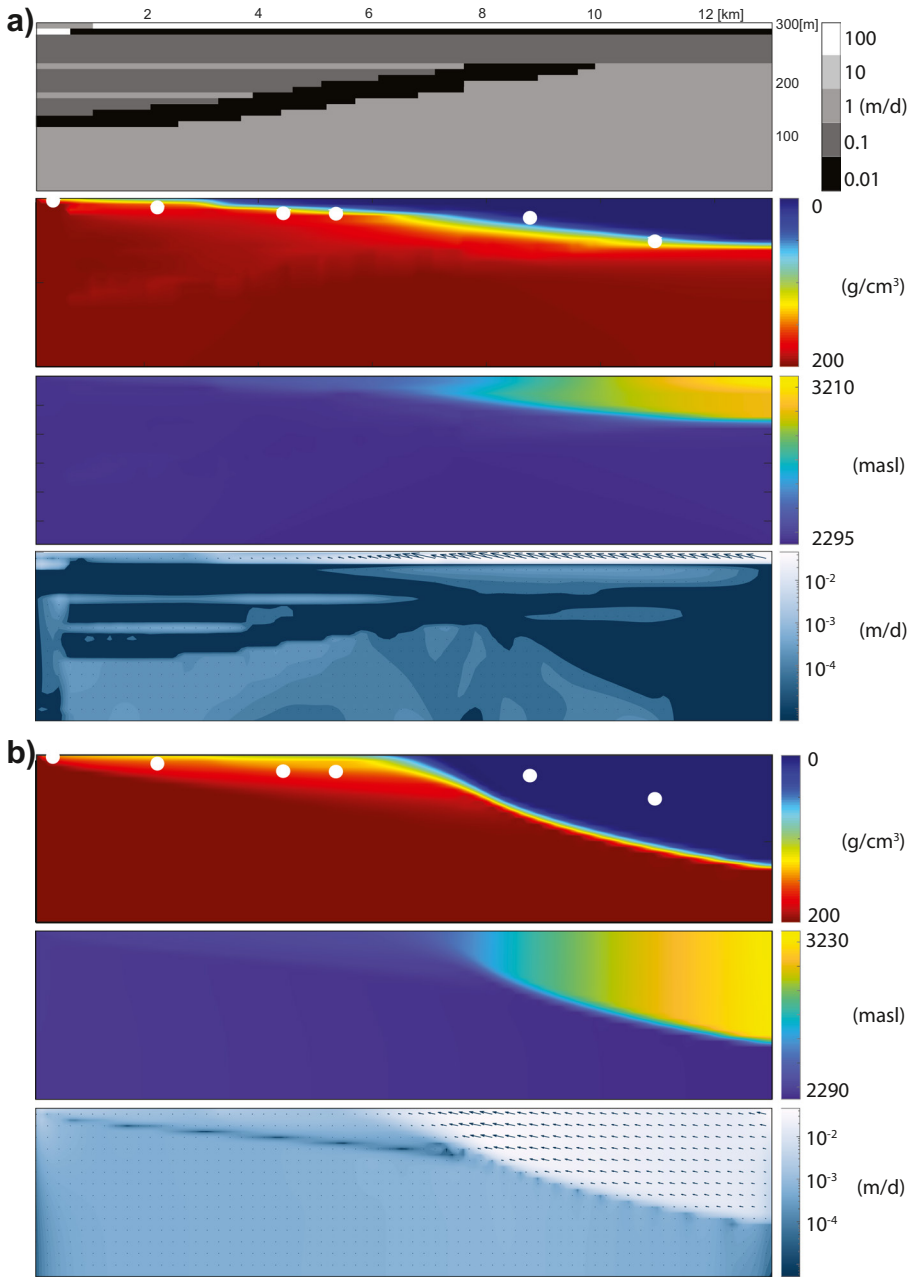

Figure 4. The distribution of hydraulic conductivity, concentration ($g \cdot cm^{-3}$) of dissolved salt, freshwater equivalent head, and flow velocity fields for both the (a) heterogeneous model based on the HSF of SdA and (b) the homogeneous model with the same K_{eff} within the 300 m by 13,000 m domain. White dots indicate the location of the observed interface in the wells along the A-A′ transect.

for each group of realizations increases by approximately half a degree for every increase in c_h/c_v by a factor of one. Homogeneous models with equivalent K_{eff} produce interface geometries that are steeper by at least a factor of two and in some cases by an order of magnitude. Figure 7 is the average and standard deviation for the horizontal width of the interface for every realization as separated by every group of realizations. Similarly, the horizontal width of the transition zone between saline and freshwater also has a pattern of decreasing while expressing more variation in the physical extent of concentration gradients as horizontal continuity increases. The homogeneous models comparatively show a consistently thicker transition zone (Figure 7).

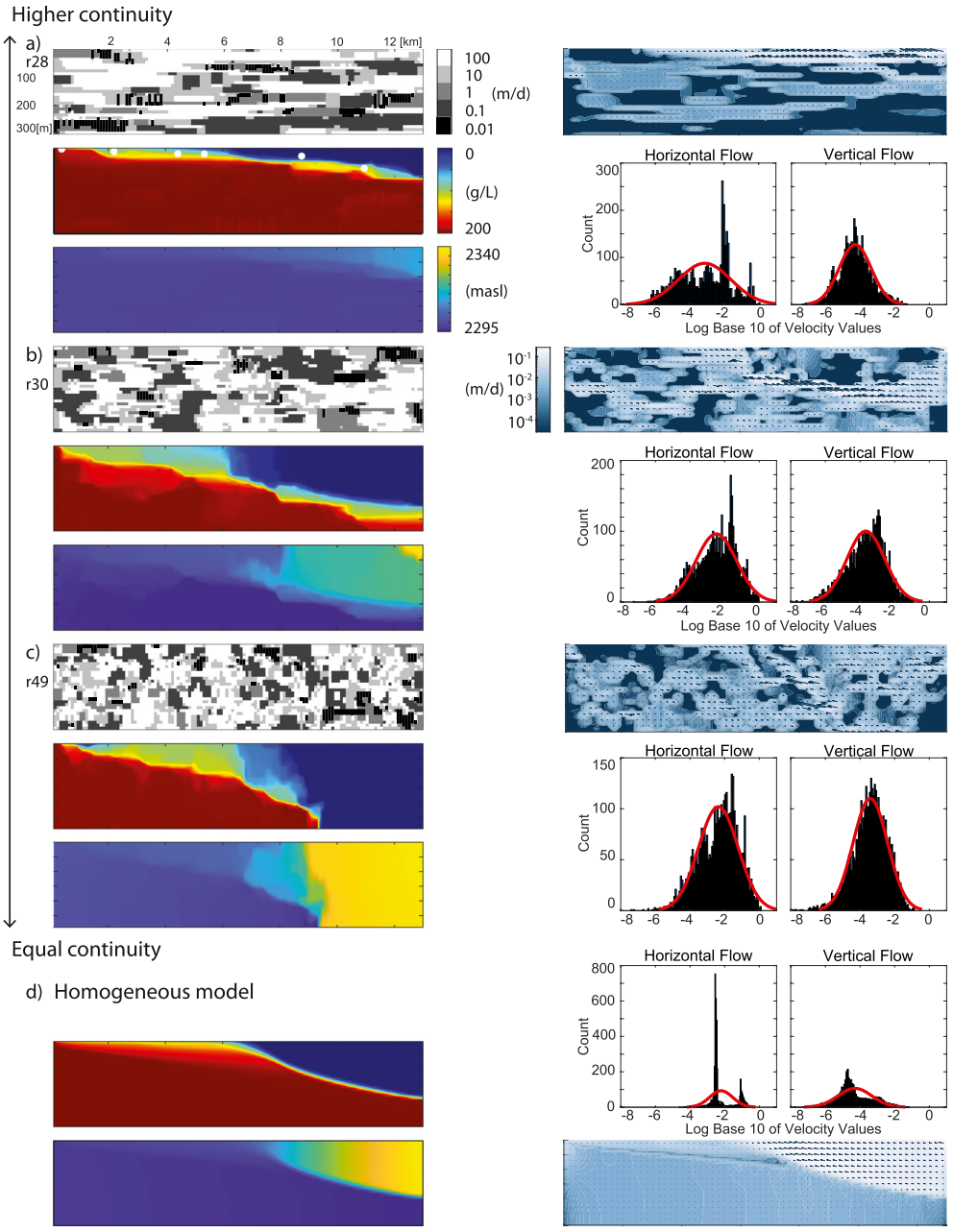

Figure 5. Results for one example of each group of K realizations in the 300 m by 13,000 m domain, with (a) $c_h/c_v = 3$, (b) $c_h/c_v = 2$, (c) $c_h/c_v = 1$, and (d) homogeneous model. For each example, clockwise from the upper left corner, the K distribution in m/d, flow velocity vectors, flow velocity distribution ($\log_{10}$ m/d), freshwater equivalent head distribution (masl), and salinity distributions (g/L) are shown. White points are observed interface locations.

The density-dependent dynamics of the realizations respond to recharge perturbations in several remarkable patterns when distinguished by c_h/c_v. Figure 8 provides the range of results for both the maximum distance traveled and the time constant value which indicates the time-sensitive response for the interface's movement following a perturbation in recharge. In these chaotic flow fields, the relatively higher velocity values are both elongated and concentrated toward the surface as c_h/c_v increases and the interface geometry shallows. The homogeneous simulation comparatively exhibits a bimodal distribution of velocity magnitudes that diverges from the heterogeneous simulations which approach Lagrangian distributions, though increased c_h/c_v exhibits more shallow freshwater upwelling that produces high concentrations of high-velocity values (Figure 5). Results further indicate that increased c_h/c_v yields an increase in the overall length

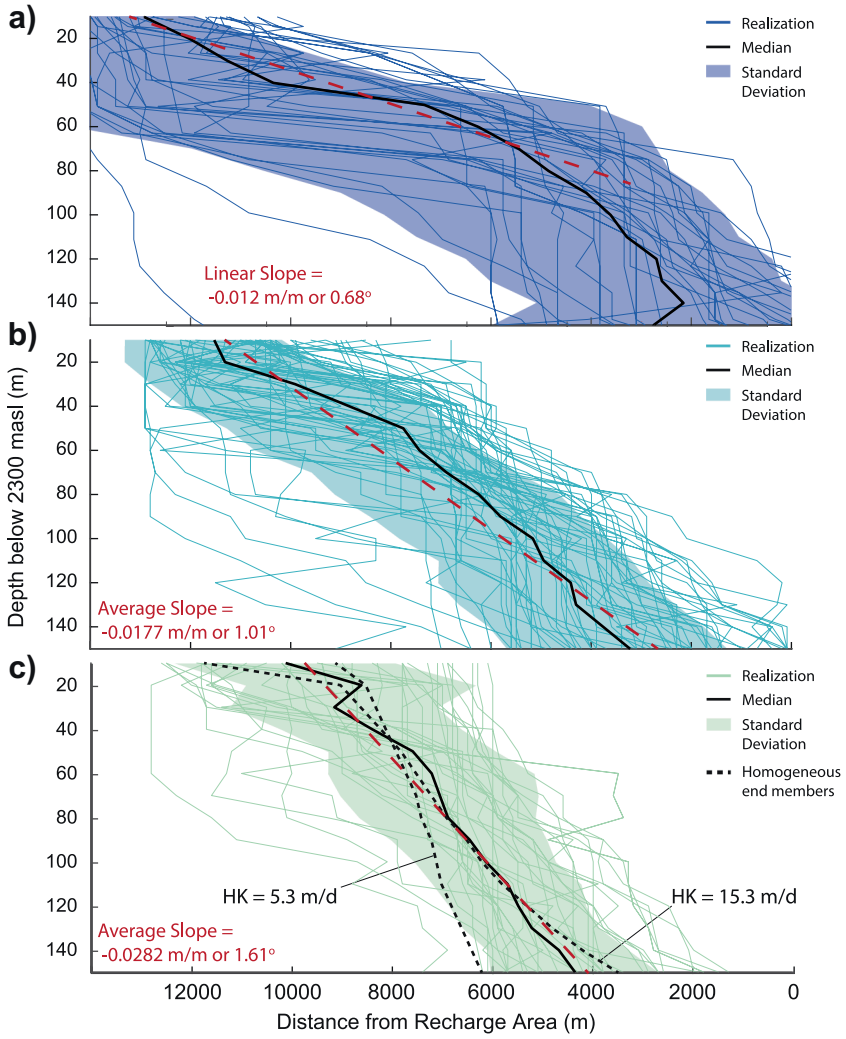

Figure 6. Distance of the 0.5 concentration point from the recharge area with depth for each group of realizations of hydraulic conductivity. Each group of realizations is separated based on degree of continuity, with increased horizontal continuity by a factor of three (dark blue), increased horizontal continuity by two (light blue), and equal continuity (green) respectively shown from top to bottom. The value for the linear best fit (dashed red) for the median (solid black) of each group is listed in the lower right corner of the graphs. The shaded region is the standard deviation.

of interface migration and thus presumably creates an increase in the response of density-dependent flow to changes in subsurface lateral inflow into an aquifer. An increase in the horizontal continuity also results in longer time constants in the exponential decay of an interface's migration rate (Figure 8). From least to most continuous, each group of realizations respectively yielded average interface migration of 3,586 ± 2,323 m, 3,816 ± 1,679 m, and 6,548 ± 2,926 m following a decrease in recharge. This equals an increase of 48% and 31% in average migration for each respective increase in c_h/c_v. For e-folding times in the interface response, the average time constant was 4804 years, 5754 years, and 9881 years for each group from least to most in c_h/c_v, creating a 20% and 72% increase in time for each respective increase in c_h/c_v. The observed time response differences are statistically significant between the groups $c_h/c_v = 1$ and $c_h/c_v = 3$ to a significance level of 0.1; between groups $c_h/c_v = 1$ versus $c_h/c_v = 3$ and $c_h/c_v = 2$ and $c_h/c_v = 3$ to a significance level of 0.05 (Table S4). Comparatively, the brine-to-freshwater interface migration within the homogeneous models exhibit less sensitivity in terms of the amount of interface movement and decreased time required to reach a new steady state subsequent to being exposed to the same perturbations in recharge.

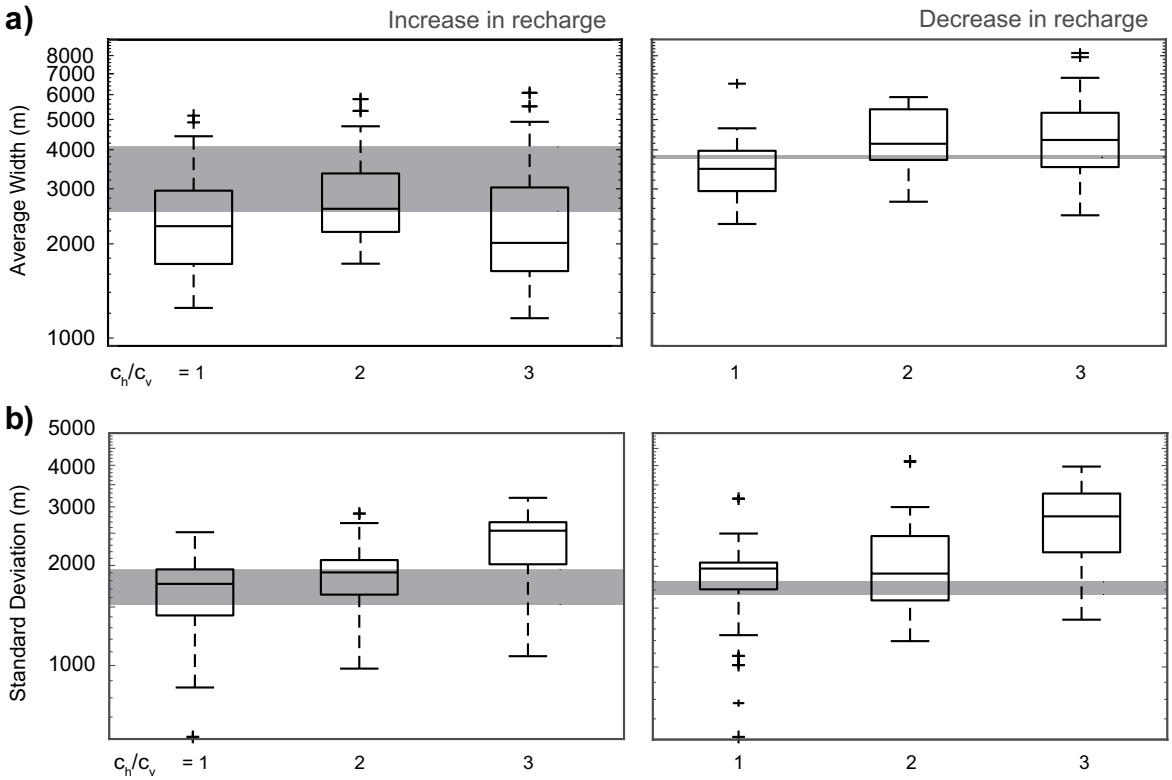

Figure 7. The distribution of (a) the average and (b) the standard deviation of transition zone widths from brackish (0.04 g·cm^{-3}) to brine (0.18 g·cm^{-3}) for the geostatistical realizations of hydraulic conductivity, separated based on c_h/c_v. Gray shaded area is the range of homogeneous values.

5. Discussion

5.1. Geometry & Inferred Density-Driven Dynamics of the Brine-to-Freshwater Interface at Salar de Atacama

This study represents the most robust attempt to date to numerically simulate and accurately capture the

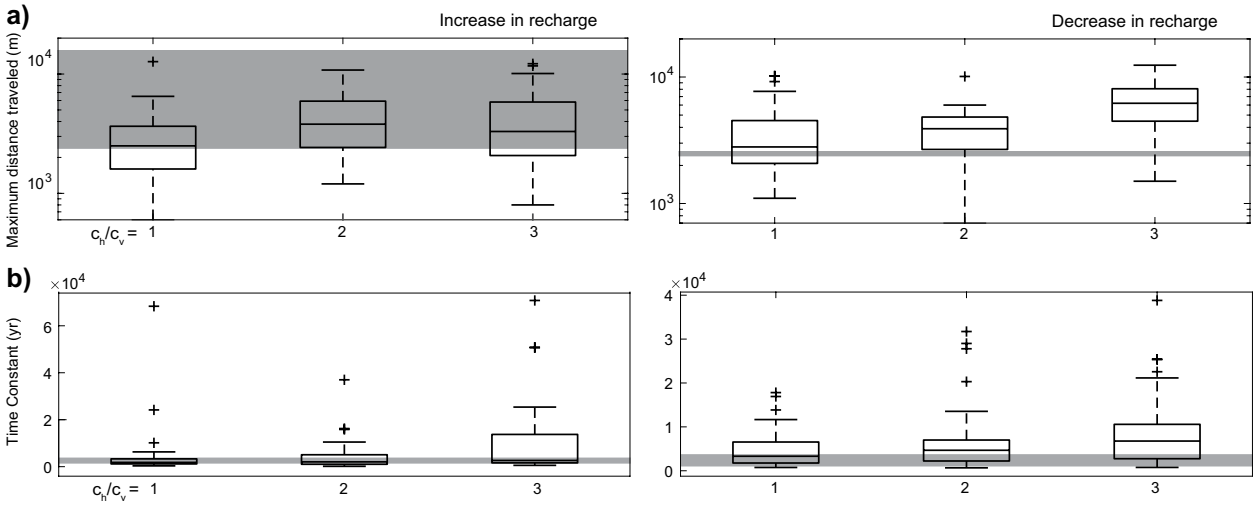

Figure 8. The distribution of (a) maximum distance of interface travel and (b) response time to a change in inflow for the geostatistical realizations of hydraulic conductivity, separated based on c_h/c_v. Above statistical analysis represent an increase in inflow and the lower plots represent results from a decrease in inflow. The gray shaded area indicates the homogeneous model results.

geometry of the brine-to-freshwater interface along the southeastern margin of the halite nucleus at SdA. It also represents the most accurate 2-D hydrostratigraphic interpretation of the southeastern margin. Simulation results of the hydraulic conductivity field resulting from the hydrostratigraphic interpretation suggest that subsurface heterogeneity impacts density-dependent dynamics to the degree that it decreases the slope the interface geometry. The increased hydrostratigraphic continuity in heterogeneous framework also focuses flow where the interface intersects conduits of relatively higher hydraulic conductivity. Focused discharge represented by the modeled velocity values occur along highly continuous preferential pathways, as shown in the results of the HSF simulation in Figure 4 and example simulations in Figure 5, further suggesting that continuity in hydrostratigraphic units may serve as a controlling factor in the impact of heterogeneity. These results therefore provide a basis for investigating not only the role of heterogeneity in hydraulic conductivity, but specifically the degree to which hydraulic conductivity differences impact density-dependent dynamics and associated solute transport. While the motivations behind previous simulations of the basin may not have included the creation of an accurate density-dependent basin-scale simulation, results from this study suggest that locating and defining the distribution of hydraulic conductivity holds value in defining density-dependent dynamics (Marazuela et al., 2018). Thus site-specific observations ostensibly indicate a possible relationship between heterogeneity in hydraulic conductivity and density-dependent sensitivity to perturbations in recharge that require further investigation, as this current work presents.

5.2. Impact of Increased Hydrostratigraphic Continuity in Heterogeneity on Density-Driven Dynamics & Resulting Interface Sensitivity

Results from the series of realizations of hydraulic conductivity demonstrate that horizontal continuity in hydrostratigraphic heterogeneity decreases the slope of the brine-to-freshwater interface (Figure 6). The simulations also support that increased horizontal continuity in hydrostratigraphic units generally decrease the average thickness of the transition zone, while also increasing the variability between a sharp and diffuse transition zone (Figure 7). Figure 9 plots the spatial distributions of OW values as a metric for characterizing flow topology for the three simulations previously shown in Figure 5. As shown in Figure 9, the shallower expression of interface slope that occurs with increasing c_h/c_v correlates with decreased vorticity-dominated flow throughout the aquifer. This supports previous findings of variable expressions of the geometry of the brine-to-freshwater interface in heterogeneous media (Michael et al., 2016). Increased variability in transition zone thickness likely results from increased preferential pathways in the horizontal direction, which is supported by the increased prevalence of strain-dominated flow in areas where the interface intersects conduits of relatively higher hydraulic conductivity (Figure 9). Since increased versus decreased perturbations in recharge have distinct effects on the thickness of the transition zone, it is important to account for different mechanisms involved in the physical expression of an interface. Increased recharge does not impact the average transition zone width because the majority of interface movement is controlled by the interplay between pressure and density gradients; decreased recharge results exhibit similar average transition zone thickness regardless of horizontal hydrostratigraphic continuity because diffusion is a primary mechanism for solute transport.

The simulated interface responses to changes in inflow are consistent with previous density-dependent interface modeling where the interface responded to hydraulically driven flow variations (Liu et al., 2014; Yechieli, 2000; Yechieli et al., 2001). This study further indicates that increased horizontal hydrostratigraphic continuity increases density-dependent sensitivity of groundwater flow in terms of the extent of interface travel and the time-sensitive response for the interface to reach a new dynamic steady state following a perturbation in recharge (Figure 8). The shift of the simulated aquifer's increased strain-dominated flow focused along the brine-to-freshwater interface as well as its variability in flow topology accounts for this change in sensitivity (Figure 9). The importance of continuity in heterogeneity is supported by comparison with homogeneous models, which have results that are comparatively limited in both length of interface movement and time-sensitive response, though they share the same K_{eff} and anisotropy values as the series of realizations of hydraulic conductivity (Figure 8). The realizations with $c_h/c_v = 1$ result in similar time responses when compared to the homogeneous results because the connectivity of vorticity-dominated flow regimes at depth allow density-dependent flow to equilibrate at comparatively similar rates. Increasing horizontal continuity in hydrostratigraphy limits the vertical connectivity of vorticity-dominated flow

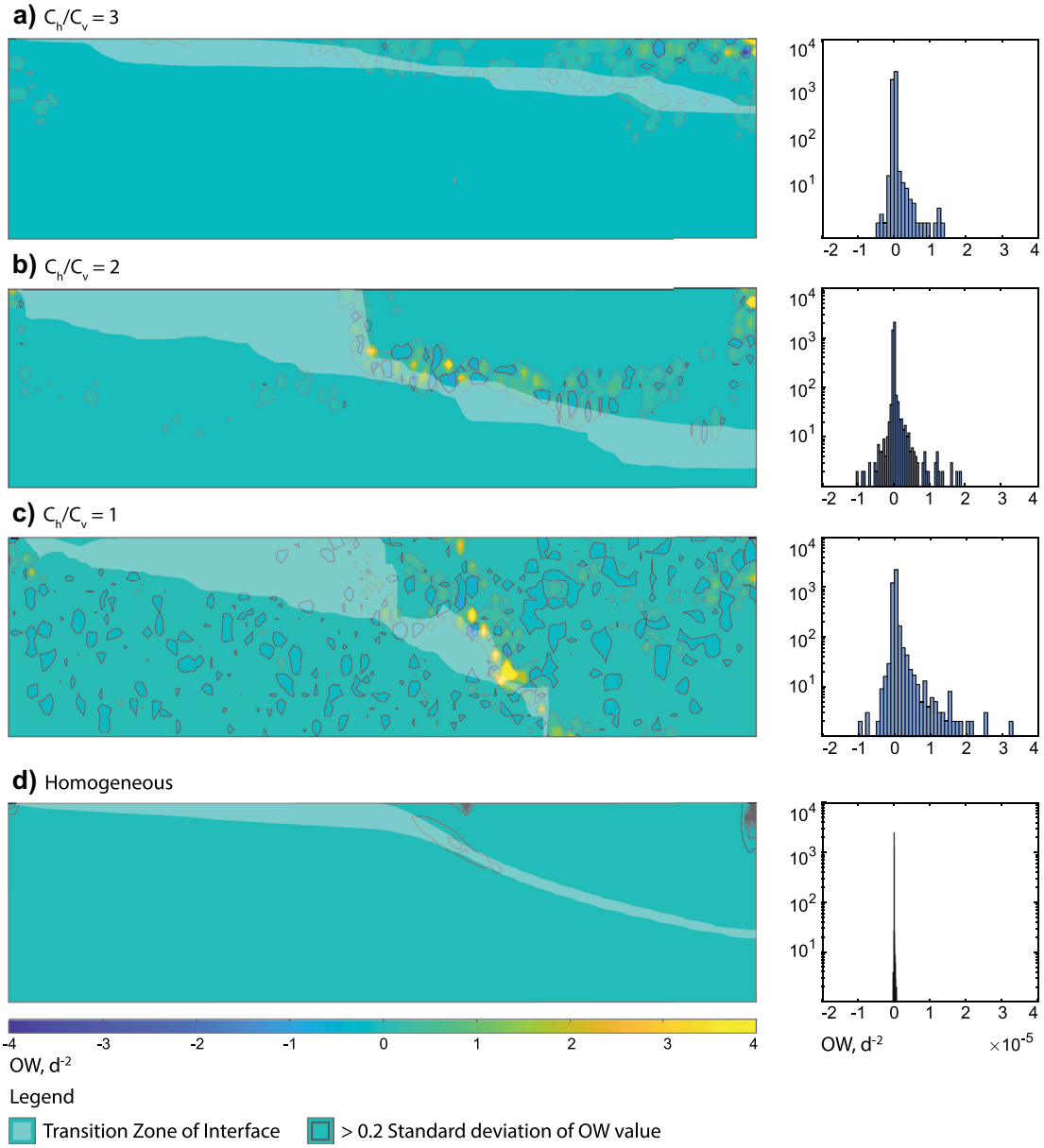

Figure 9. Spatial distributions and histograms of OW values for the same example simulations for each group from Figure 5, with (a) $c_h/c_v = 3$, (b) $c_h/c_v = 2$, (c) $c_h/c_v = 1$, and (d) homogeneous model. The white shaded areas indicate the physical location of the simulated interface's transition zone and the gray lines indicate areas where the OW increases above 0.2 of the standard deviation. OW, Okubo-Weiss.

regimes and promotes strain-dominated flow, which promotes further localization of chaotic advection and therefore results in prolonged density-driven flow responses at the aquifer scale.

Horizontal continuity in hydrostratigraphic unit controls flow topology along the brine-to-freshwater interface in density-dependent dynamics, and this relationship is responsible for the resulting variable sensitivity of the interface to recharge perturbations. An increase in c_h/c_v leads to an increase in the prevalence of highly conductive preferential pathways in the horizontal direction which thus increases the potential for localized advection in a chaotic flow field. These localized hydraulic conditions result in increased variability in pressure gradients in the vertical direction. Higher hydraulic disequilibrium therefore results in longer timescales required for density-dependent flow to reach a new stable position. Sensitivity likewise increases in terms of the length of interface migration because increased preferential pathways facilitate sensitivity to density-driven pressure variations and thus trigger strain-dominated flow where the interface meets

media with high hydraulic conductivity. OW analysis suggests that strain-dominated flow ($OW > 0.2\sigma_{OW}$) is focused along the brine-to-freshwater interface where it intersects with high-K preferential pathways (Figure 9). Physical distributions of OW values shown in Figure 9 also indicate elongated diffusion-dominated flow in the horizontal direction as c_h/c_v increases. These two observations indicate that while increased c_h/c_v creates horizontally elongated diffusive flow conditions that increase hydraulic disparities in the vertical direction and therefore decrease the response time for the system as a whole, the interface-specific locations of conduits for preferential flow host the density-dependent discrepancies in pressure gradients that drive saline intrusion.

Simulated evaporation remained constant throughout the study, and an analysis of the impact of evaporation on the brine-to-freshwater interface sensitivity is beyond the scope of this study. However, it is possible to infer the potential impact from evaporation on the interface-based sensitivity analysis. A remarkably consistent characteristic of the response to changes in inflow was the relatively unchanged interface position within the modeled area of evaporation. When the interface's confluence with the surface intersected the evaporation area, interface migration in response to perturbations in recharge decreased by almost an order of magnitude compared to the average length of migration at depth. This observation confirms the importance of considering potential evaporation in arid aquifers with abundant brine.

5.3. Implications for Future Simulations & Accurate Physical Expressions of Brine-to-Freshwater Interfaces in Arid Basins

Increased horizontal hydrostratigraphic continuity creates brine-to-freshwater interface dynamics that shallow the interface and increase the variability in transition zone thickness, which differs from predictions based on homogeneous numerical simulations of density-dependent groundwater flow (Figure 10). The direct relationship between lateral hydrostratigraphic continuity in subsurface heterogeneity and interface geometry indicates that heterogeneity represents a primary control on brine-bearing systems with subsurface lateral recharge as the primary long-term recharge mechanism. The relationship between horizontal continuity in geologic heterogeneity and variability in transition zone thickness indicates that representations of hydrostratigraphic heterogeneity is valuable for realistic expressions of the interface thickness. This is especially critical for arid endorheic basins, where the development of transitional evaporite facies creates locally continuous units (Vásquez et al., 2013). In salar environments, the prevalence of continuous boundaries of evaporite series against higher-permeability facies may account for the shallowing behavior of observed interfaces in certain locations where high evaporation dominates. Brine-bearing aquifers with continuous stratigraphic contacts between high and low permeability units may develop distinctly shallower interface geometries than traditional homogeneous or simplistic models, where units with higher hydraulic conductivity act as conduits for fluid flow. This is especially true for depositional environments and marginal zones adjacent to developed salars. These observations are particularly relevant to brine-bearing aquifers that do not experience additional hydraulic fluctuations like tidal forcing and wave-induced circulation, such as coastal aquifers.

These findings hold several implications for the future of numerically simulating density-dependent flow in arid and endorheic basins. Current density-dependent modeling of such basins typically produces simple representations of an aquifer, using homogeneous changes in anisotropy or simple layers with differing hydraulic conductivity values in order to shallow the interface geometry and match model results with observed field conditions. Considering that recharge may decrease in arid climates as a result of climate change, it is prudent to focus on the impacts of decreased inflow in the models (Wang et al., 2018). Modeling suggests that brine-to-freshwater interface migration distances are at least 10%–35% more sensitive to a decrease than an increase in inflow. These reactions highlight the importance of accounting for projected climate-driven changes in the hydrologic budgets of arid basins. Without considering the geologic complexity or continuity of hydrostratigraphic units in an aquifer, such models result in conditions that may not produce either accurate geometries or reliable saline intrusion predictions. Thus homogeneous models are not suitable for understanding an aquifer's response to climate-driven changes in recharge. While simple changes in anisotropy may produce interface slopes that approach observed conditions, they do not account for local variation in the geometry, including the observed shallowing trend seen in the upper 50 m of the aquifer of SdA. This sensitivity analysis documents that this shallowing trend impacts the time dependent

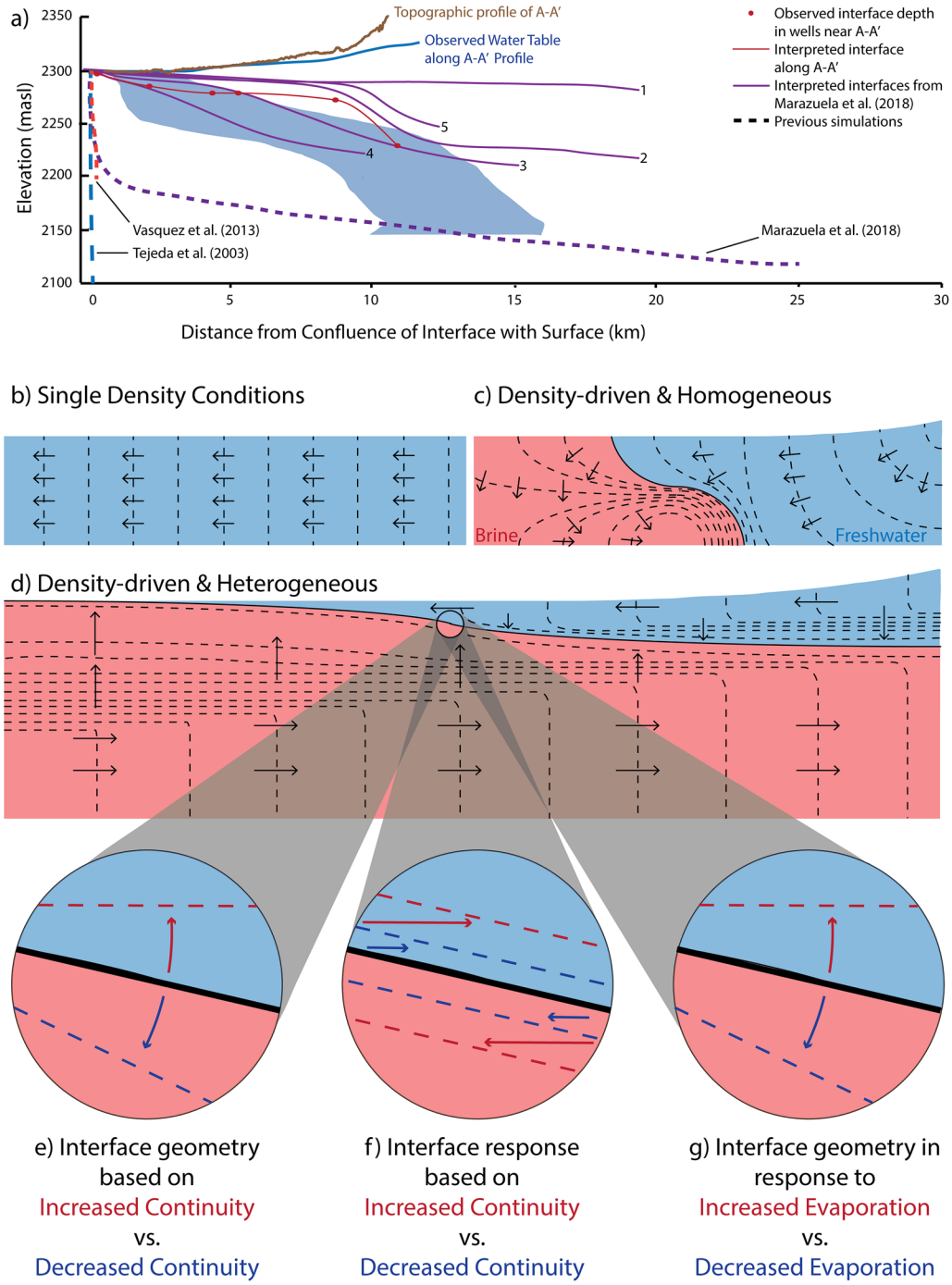

Figure 10. Conceptual illustration of results from observations of simulations with different distributions of hydraulic conductivity, with (a) a comparison of this study's simulations with previous studies, (b) a homogeneous, single-density flow with black dashed lines showing potentiometric head contours, (c) a homogeneous, variable-density flow model where the main determinant of interface geometry is the difference in density, and (d) a heterogeneous model where the geometry of the interface is dependent on density. (e) The extent of continuity in K influences interface geometry. (f) The sensitivity of the interface is also sensitive to continuity. (g) The extent and rate of evaporation also has a likely impact on interface geometry.

density-driven response to changes in inflow. Accurate estimations of saline intrusion therefore require precise modeling of geologic heterogeneity in order to more effectively assess geometry as well as response to changes in recharge and discharge mechanisms. Since, high horizontal continuity is a common feature in sedimentary deposits, such as salars specifically, and arid, endorheic basins in general, homogeneous or simplistic modeling methods underestimate both the total amount of possible saline intrusion and the timescale at which migration can occur. This implies that predictions and analysis of transient saline intrusion in all brine-bearing aquifers must account for subsurface heterogeneity, especially within interface-adjacent areas.

5.4. Limitations of the Simulation Framework

Randomized distributions of hydraulic conductivity may not exactly represent the asymmetrical depositional environments of salt flats. Evaporite sequences produce geochemically zoned areas that often abut facies with distinctly different hydrogeologic characteristics (Vásquez et al., 2013). This creates an asymmetric distribution of hydraulic properties, which randomized distributions of hydraulic conductivity may not accurately represent. Therefore, analysis of time constant values is limited to comparison among models. While a simple comparison with the HSF model indicates that most of the time constant values may seem plausible for salar environments, the question of the realizations' geologic plausibility impedes the ability to rely on time constant values produced from these models as globally realistic scenarios.

Several hydrogeologic conditions remain homogeneous in the framework for the simulations, despite their direct correlation to changes in hydraulic conductivity. Specific yield, porosity, and anisotropy would be intrinsically heterogeneous, yet they remain consistently homogeneous for computational simplicity given the number of realizations in the study's scope. Constant and homogeneous values for these variables may under-represent the full impact of subsurface heterogeneity on the hydrogeologic dynamics of these aquifers.

6. Conclusion

Constraining the physical impacts of heterogeneity of hydraulic conductivity on the density-driven dynamics that control brine-to-freshwater interface migration and sensitivity is crucial for managing groundwater resources of brine-bearing aquifers in anticipation of climate-driven change. Homogeneous numerical simulations of density-driven flow fail to capture accurate geometry and presumably the dynamics of such interfaces. Aiming to develop a more accurate framework for the mechanisms driving density-driven fluid flow in arid basins, we assess the extent to which lateral hydrostratigraphic continuity impacts physical characteristics and time-sensitive behavior of the interface. To constrain the impact of continuity in geologic complexity, we employ a series of realizations of hydraulic conductivity with varying horizontal continuity. Following a perturbation in the simulated recharge to groundwater flow through each realization, we collect the interface slope, total distance that the interface travels, and the time required for the interface to reach a new steady-state in terms of an “e-folding” time constant.

The hydraulic conductivity distribution from the hydrostratigraphic framework of SdA produced a modeled interface that matched the observed location within 10 m to a depth of 100 m. Solute distribution results from the homogeneous counterpart of the HSF diverged from observed values. Simulated responses to perturbations in recharge from the HSF were also longer in both interface migration and migration response times than the homogeneous results. Results from the series of realizations of hydraulic conductivity distributions investigate whether the comparative observations can be attributed to hydrostratigraphic continuity in heterogeneity. Simulated values of concentration best match observed conditions from SdA for the realizations with the strongest trend in horizontal continuity. Results further show a decrease in the slope of the interface as horizontal hydrostratigraphic continuity increases in the heterogeneous realizations, indicating that the improved matching of observed and simulated values is linked to the shallowing effect of increased continuity. This suggests that the relationship between the different hydrostratigraphic units and the resulting localized disequilibrium from those preferential pathways controls the distribution and sensitivity of the interface to recharge perturbations. Our findings show a relationship between hydrostratigraphic continuity in heterogeneous environments and the resulting brine-to-freshwater interface response dynamics,

with interface migration increasing by an order of magnitude and migration response times increasing by a factor of three when horizontal hydrostratigraphic continuity increases by a factor of two.

The results suggest that horizontal hydrostratigraphic continuity in heterogeneity impacts saline intrusion and therefore must be accounted for when modeling at the basin scale. The degree to which both anthropogenic extraction and evaporation coupled with hydrostratigraphic continuity impact interface dynamics remains undefined in arid basins. Future modeling initiatives using a similar geostatistical approach can address possible relationships on these different strains to brine-bearing aquifers. Arid regions throughout the world are experiencing strains on groundwater resources as anthropogenic exploitation and climate-driven aridity increases. This modeling approach constrains the density-driven dynamics of brine-to-freshwater interfaces in arid regions in response to climate-driven changes in recharge by establishing a first-order control between hydrostratigraphic continuity and density-driven dynamics. This study also confirms the importance of subsurface heterogeneity in controlling time-sensitive reactions to changes in recharge for all brine-bearing aquifers.

Data Availability Statement

The data and model results presented may be obtained through the University of Massachusetts Data Repository.

Acknowledgments
The authors would like to thank the Albemarle Corporation for supporting our ongoing research in order to further develop the understanding of density-driven flow dynamics. Special thanks to J. Garcia for his acumen and encouragement of our work. Funding for this work was primarily provided by Albemarle Corporation and research on the sediment cores was supported by the National Science Foundation (grant number EAR1443226).

References

Bailey, R. (2015). Quantifying transient post-overwash aquifer recovery for atoll islands in the western Pacific. *Hydrological Processes*, *29*, 4470–4482.

Bear, J. (1972). *Dynamics of fluids in porous media* (Vol. 53). New York, NY: Elsevier Science.

Boutt, D. F., Hynek, S. A., Munk, L. A, & Corenthal, L. G. (2016). Rapid recharge of fresh water to the halite-hosted brine aquifer of Salar de Atacama, Chile. *Hydrological Processes*, *30*, 4720–4740.

Carle, S. (1999). *T-PROGS: Transition probability geostatistical software* (pp. 1–78). Davis, CA: University of California.

Carmona, V., Pueyo, J. J., Taberner, C., Chong, G., & Thirlwall, M. (2000). Solute inputs in the Salar de Atacama (N. Chile). *Journal of Geochemical Exploration*, *69–70*, 449–452.

Condon, L. E., & Maxwell, R. M. (2019). Simulating the sensitivity of evapotranspiration and streamflow to large-scale groundwater depletion. *Science Advances*, *5*, 1–9.

Corenthal, L., Boutt, D. F., Hynek, S., & Munk, L. A. (2016). Regional groundwater flow and accumulation of a massive evaporite deposit at the margin of the Chilean Altiplano. *Geophysical Research Letters*, *43*(15), 8017–8025. https://doi.org/10.1002/2016GL070076

de Barros, F., Dentz, M., Koch, J., & Nowak, W. (2012). Flow topology and scalar mixing in spatially heterogeneous flow fields. *Geophysical Research Letters*, *39*, 1–5. https://doi.org/10.1029/2012GL051302

Duffy, J., & Hassan, S. (1988). Groundwater circulation in a closed desert basin: Topographic scaling and climatic forcing. *Water Resources Research*, *24*(10), 1675–1688.

Eugster, H. P. (1980). Geochemistry of evaporitic lacustrine deposits. *Annual Review of Earth and Planetary Sciences*, *8*, 35–63.

Fan, Y., Duffy, C., & Oliver, D. (1996). Density-driven groundwater flow in closed desert basins: Field investigations and numerical experiments. *Journal of Hydrology*, *196*, 139–184.

Ferguson, G., & Gleeson, T. (2012). Vulnerability of coastal aquifers to groundwater use and climate change. *Nature Climate Change*, *2*, 342–345.

Gelhar, L. W., Welty, C., & Rehfeldt, K. R. (1992). A critical review of data on field-scale dispersion in aquifers. *Water Resources Research*, *28*(7), 1955–1974.

Geng, X., & Boufadel, M. C. (2015). Impacts of evaporation on subsurface flow and salt accumulation in a tidally influenced beach. *Water Resources Research*, *51*, 5547–5565. https://doi.org/10.1002/2015WR016886

Geng, X., Boufadel, M. C., Rajaram, H., Cui, F., Lee, K., & An, C. (2020). Numerical study of solute transport in heterogeneous beach aquifers subjected to tides. *Water Resources Research*, *56*, 1–20. https://doi.org/10.1029/2019WR026430

Haitjema, H. M., & Mitchell-Bruker, S. (2005). Are water tables a subdued replica of the topography? *Ground Water*, *43*(6), 781–786.

Heiss, J., & Michael, H. A. (2014). Saltwater-freshwater mixing dynamics in a sandy beach aquifer over tidal, spring-neap, and seasonal cycles. *Water Resources Research*, *50*, 6747–6766. https://doi.org/10.1002/2014WR015574

Heiss, J., Michael, H. A., & Koneshloo, M. (2020). Denitrification hotspots in intertidal mixing zones linked to geologic heterogeneity. *Environmental Research Letters*, *15*(8), 084015. https://doi.org/10.1088/1748-9326/ab90a6

Heiss, J., Post, V., Laattoe, T., Russoniello, C., & Michael, H. (2017). Physical controls on biogeochemical processes in intertidal zones of beach aquifers. *Water Resources Research*, *53*, 9225–9244. https://doi.org/10.1002/2017WR021110

Held, R., Attinger, S., & Kinzelbach, W. (2005). Homogenization and effective parameters for the Henry problem in heterogeneous formations. *Water Resources Research*, *41*(11), 1–14. https://doi.org/10.1029/2004WR003674

Hernández-López, M. F., Gironás, J., Braud, I., Suárez, F., & Muñoz, J. F. (2014). Assessment of evaporation and water fluxes in a column of dry saline soil subject to different water table levels. *Hydrological Processes*, *28*, 3655–3669.

Houston, J. (2009). A recharge model for high altitude, arid, Andean aquifers. *Hydrological Processes*, *23*, 2383–2393.

Houston, J., Butcher, A., Ehren, P., Evans, K., & Godfrey, L. (2011). The evaluation of brine prospects and the requirement for modifications to filing standards. *Economic Geology*, *106*(7), 1125–1239.

Jazayeri, A., Werner, A. D., Wu, H., & Lu, C. (2020). Effects of river partial penetration on the occurrence of riparian freshwater lenses: Theoretical development. *Water Resources Research*, *56*(10), 1–17. https://doi.org/10.1029/2020WR027786

Jordan, T. E., Mpodozis, C., Muñoz, N., Blanco, N., Pananont, P., & Gardeweg, M. (2004). Cenozoic subsurface stratigraphy and structure of the Salar de Atacama basin, northern Chile. *Journal of South American Earth Sciences*, *23*, 122–146.
Jordan, T. E., Muñoz, N., Hein, M. C., Lowenstein, T., Godfrey, L., & Yu, J. (2002). Active faulting and folding without topographic expression in an evaporite basin, Chile. *Bulletin of the Geological Society of America*, *114*(11), 1406–1421.
Kerrou, J., & Renard, P. (2010). Analyse numérique des effets dimensionnels et des hétérogénéités sur les intrusions d'eau marine en milieu dispersif. *Hydrogeology Journal*, *18*(1), 55–72. https://doi.org/10.1007/s10040-009-0533-0
Kesler, S. E., Gruber, P. W., Medina, P. A., Keoleian, G. A., Everson, M. P., & Wallington, T. J. (2012). Global lithium resources: Relative importance of pegmatite, brine and other deposits. *Ore Geology Reviews*, *48*, 55–69. https://doi.org/10.1016/j.oregeorev.2012.05.006
Ketabchi, H., Mahmoodzadeh, B., Ataie-Ashtiani, B., & Simmons, C. (2016). Sea-level rise impacts on seawater intrusion in coastal aquifers: Review and integration. *Journal of Hydrology*, *535*, 235–255.
Klammler, H., Jawitz, J., Annable, M., Yaquain, J. A., Hatfield, K., & Burger, P. (2020). Decadal scale recharge-discharge time lags from aquifer freshwater-saltwater interactions. *Journal of Hydrology*, *582*, 1–13. https://doi.org/10.1016/j.jhydrol.2019.124514
Konikow, L. F., Akhavan, M., Langevin, C. D., Michael, H. A., & Sawyer, A. H. (2013). Seawater circulation in sediments driven by interactions between seabed topography and fluid density. *Water Resources Research*, *49*(3), 1386–1399.
Kreyns, P., Geng, X., & Michael, H. A. (2020). The influence of connected heterogeneity on groundwater flow and salinity distributions in coastal volcanic aquifers. *Journal of Hydrology*, *586*, 1–10. https://doi.org/10.1016/j.jhydrol.2020.124863
Kunasz, I. A. (1980). *Lithium in brines.* Paper presented at Fifth Symposium on Salt (Vol. 1, pp. 115–117).
Langevin, C., & Guo, W. (2006). Modflow/mt3dms—based simulation of variable-density ground water flow and transport. *Ground Water*, *44*(3), 339–351.
Liu, Y., Mao, X., Chen, J., & Barry, D. (2014). Influence of a coarse interlayer on seawater intrusion and contaminant migration in coastal aquifers. *Hydrological Processes*, *28*, 5162–5175.
Lowenstein, T. K., Hein, M. C., Bobst, A. L., Jordan, T. E., Ku, T. L., & Luo, S. (2003). An assessment of stratigraphic completeness in climate-sensitive closed-basin lake sediments: Salar de Atacama, Chile. *Journal of Sedimentary Research*, *73*(1), 91–104.
Mahmoodzadeh, D., & Karamouz, M. (2019). Seawater intrusion in heterogeneous coastal aquifers under flooding events. *Journal of Hydrology*, *568*, 1118–1130. https://doi.org/10.1016/j.jhydrol.2018.11.012
Marazuela, M., Vázquez-Suñé, E., Custodio, E., Palma, T., Garcia-Gil, A., & Ayora, C. (2018). Projections to the superior colliculus from inferior parietal, ventral premotor, and ventrolateral prefrontal areas involved in controlling goal-directed hand actions in the macaque. *Journal of Hydrology*, *561*, 223–235.
Maxey, G. B. (1968). Hydrogeology of desert basins. *Ground Water*, *6*(5), 10–22.
Meng, G., Han, Y., Wang, S., & Wang, Z. (2002). Seawater intrusion types and regional divisions in the southern coast of Laizhou bay. *Chinese Journal of Oceanology and Limnology*, *20*(3), 277–284.
Michael, H. A., & Khan, M. R. (2016). Impacts of physical and chemical aquifer heterogeneity on basin-scale solute transport: Vulnerability of deep groundwater to arsenic contamination in Bangladesh. *Advances in Water Resources*, *98*, 147–158.
Michael, H. A., Scott, K. C., Koneshloo, M., Yu, X., Khan, M. R., & Li, K. (2016). Geologic influence on groundwater salinity drives large seawater circulation through the continental shelf. *Geophysical Research Letters*, *43*(10), 782–791. https://doi.org/10.1002/2016GL070863
Montgomery, E. L., Rosko, M. J., Castro, S. O., Keller, B. R., & Bevacqua, P. S. (2003). Interbasin underflow between closed Altiplano basins in Chile. *Ground Water*, *41*(4), 523–531.
Morgan, L., Werner, A., & Simmons, C. (2012). On the interpretation of coastal aquifer water level trends and water balances: A precautionary note. *Journal of Hydrology*, *470–471*, 280–288.
Mpodozis, C., Arriagada, C., Basso, M., Roperch, C., & Reich, M. (2005). Late mesozoic to paleogene stratigraphy of the Salar de Atacama basin, Antofagasta, northern Chile: Implications for the tectonic evolution of the central Andes. *Tectonophysics*, *399*, 125–154.
Munk, L. A., Boutt, D., Moran, B. J., McKnight, S. V., & Jenckes, J. (2020). Hydrogeologic and geochemical distinctions in Salar freshwater brine systems. *Geochemistry, Geophysics, Geosystems*, *22*, e2020GC009345. https://doi.org/10.31223/osf.io/j3pu6
Munk, L. A., Boutt, D. F., Hynek, S. A., & Moran, B. (2018). Hydrochemical fluxes and processes contributing contributing to the formation of lithium-enriched brines in a hyper-arid continental basin. *Chemical Geology*, *493*, 37–57. https://doi.org/10.1016/j.chemgeo.2018.05.013
Munk, L. A., Hynek, S. A., Bradley, D. A., Boutt, D. F., Labay, K., & Jochens, H. (2016). Lithium brines: A global perspective. *Reviews in Economic Geology*, *18*, 339–365.
Okubo, A. (1970). Horizontal dispersion of floatable particles in the vicinity of velocity singularities such as convergences. *Deep-Sea Research and Oceanographic Abstracts*, *17*(3), 445–454. https://doi.org/10.1016/0011-7471(70)90059-8
Ortiz, C., Aravena, R., Briones, E., Suárez, R., Tore, C., & Muñoz, J. F. (2014). Sources of surface water for the soncor ecosystem, Salar de Atacama basin, northern Chile. *Hydrological Sciences Journal*, *59*(2), 336–350.
Philip, J. R., & van Duijn, C. J. (1996). Slumping of brine mounds: Bounds on behaviour. *Journal of Hydrology*, *179*, 159–180.
Placzek, C., Quade, J., Betancourt, J. L., Patchett, P. J., Rech, J. A., Latorre, C., et al. (2009). Climate in the dry central Andes over geologic, Millenial, and interannual timescale. *Annals of the Missouri Botanical Garden*, *96*(3), 386–397.
Pool, M., Post, V. E., & Simmons, C. T. (2015). Reply to comment by Behzad Ataie-Ashtiani on "effects of tidal fluctuations on mixing and spreading in coastal aquifers: Homogeneous Case", *Water Resources Research*, *51*(6), 4859–4860. https://doi.org/10.1002/2015WR017111
Post, V., Galvis, S. C., Sinclair, P. J., & Werner, A. D. (2019). Evaluation of management scenarios for potable water supply using script-based numerical groundwater models of a freshwater lens. *Journal of Hydrology*, *571*, 843–855.
Post, V., Houben, J. G., & van Engelen, J. (2018). What is the Ghijben-Herzberg principle and who formulated it? *Hydrogeology Journal*, *26*(6), 1801–1807.
Post, V., Kooi, H., & Simmons, C. (2007). Using hydraulic head measurements in variable-density ground water flow analyses. *Ground Water*, *45*(6), 664–671.
Qureshi, A. S. (2011). Water management in the Indus basin in Pakistan: Challenges and opportunities. *Mountain Research and Development*, *31*, 3.
Reutter, K. J., Charrier, R., Götze, H. J., Schurr, B., Wigger, P., Scheuber, E., et al. (2006). *The Salar de Atacama basin: A subsiding block within the western edge of the Altiplano-Puna plateau*. In Andes: Active Subduction Orogeny (pp. 303–325). Springer.
Rissman, C., Leybourne, M., Benn, C., & Christenson, B. (2015). The origin of solutes within the groundwaters of a high Andean aquifer. *Chemical Geology*, *396*, 164–181.
Rosen, M. (1994). *The importance of groundwater in playas: A review of playa classifications and the sedimentology and hydrology of playas*. In Geological Society of America Special Papers (p. 289).

Russoniello, C. J., Fernandez, C., Bratton, J. F., Banaszak, J. F., Krantz, D. E., Andres, A. S., et al. (2013). Geologic effects on groundwater salinity and discharge into an estuary. *Journal of Hydrology*, *498*, 1–12.

Sanford, W. E., & Pope, J. P. (2010). Current challenges using models to forecast seawater intrusion: Lessons from the eastern shore of Virginia, USA. *Hydrogeology Journal*, *18*(1), 73–93.

Sawyer, A., Lazareva, O., Kroeger, K. D., Crespo, K., Chan, C. S., Stieglitz, T., & Michael, H. (2014). Stratigraphic controls on fluid and solute fluxes across the sediment-water interface of an estuary. *Limnology & Oceanography*, *59*, 997–1010. https://doi.org/10.4319/lo.2014.59.3.0997

Scanlon, B. R., Keese, K. E., Flint, A. L., Flint, L. E., Gaye, C. B., Edmunds, W. M., & Simmers, I. (2006). Global synthesis of groundwater recharge in semiarid and arid regions. *Hydrological Processes*, *20*, 3335–3370.

Schaller, M. F., & Fan, Y. (2009). River basins as groundwater exporters and importers: Implications for water cycle and climate modeling. *Journal of Geophysical Research*, *114*, 1–20. https://doi.org/10.1029/2008JD010636

Schincariol, A., Schwartz, F., & Mendoza, C. (1997). Instabilities in variable density flows: Stability and sensitivity analyses for homogeneous and heterogeneous media. *Water Resources Research*, *33*, 31–41. https://doi.org/10.1029/96WR02587

Stein, V., Yechieli, Y., Shalev, E., Kasher, R., & Sivan, O. (2019). The effect of pumping saline groundwater for desalination on the fresh-saline water interface dynamics. *Water Research*, *157*, 46–57.

Steinmetz, R. L. L. (2017). Lithium- and boron-bearing brines in the Central Andes: Exploring hydrofacies on the eastern Puna plateau between 23° and 23°30′S. *Mineralium Deposita*, *52*, 35–50. https://doi.org/10.1007/s00126-016-0656-x

Tejeda, I., Cienfuegos, R., Muñoz, J. F., & Durán, M. (2003). Numerical modeling of saline intrusion in Salar de Atacama. *Journal of Hydrologic Engineering*, *8*(1), 25–34.

Trabelsi, F., Ben Mammou, A., Tarhouni, J., Piga, C., & Ranieri, G. (2013). Delineation of saltwater intrusion zones using the time domain electromagnetic method: The Nabeul-Hammamet coastal aquifer case study. *Hydrological Processes*, *27*, 2004–2020.

Tyler, S. W., Muñoz, J. F., & Wood, W. W. (2006). The response of playa and Sabkha hydraulics and mineralogy to climate forcing. *Ground Water*, *44*(3), 329–338.

Vásquez, C., Ortiz, P., Suárez, F., & Muñoz, J. (2013). Modeling flow and reactive transport to explain mineral zoning in the Atacama salt flat aquifer, Chile. *Journal of Hydrology*, *490*, 114–125.

Wang, J., Song, C., Reager, J., Yao, F., Famigletti, J. S., Sheng, Y., et al. (2018). Recent global decline in endorheic basin water storages. *Nature Geoscience*, *11*, 926–932.

Weiss, J., & Provenzale, A. (2008). *Transport and mixing in geophysical flows*. Springer

Werner, A. D., Bakker, M., Post, V. E. A., Vandenbohede, A., Lu, C., Ataie-Ashtiani, B., et al. (2013). Seawater intrusion processes, investigation and management: Recent advances and future challenges. *Advances in Water Resources*, *51*, 3–26. https://doi.org/10.1016/j.advwatres.2012.03.004

Werner, A. D., & Simmons, C. T. (2009). Impact of sea-level rise on sea water intrusion in coastal aquifers. *Ground Water*, *47*(2), 197–204.

Wooding, R. A., Tyler, S. W., & White, I. (1997). Convection in groundwater below an evaporating Salt Lake: 1. Onset of instability. *Water Resources Research*, *33*(6), 1199–1217.

Yager, R., McCoy, K., Voss, C., Sanford, W. E., & Winston, R. B. (2017). The role of uplift and erosion in the persistence of saline groundwater in the shallow subsurface. *Geophysical Research Letters*, *98*, 147–158.

Ye, M., Wang, L., Pohlmann, K. F., & Chapman, J. B. (2016). Evaluating groundwater interbasin flow using multiple models and multiple types of data. *Ground Water*, *54*(6), 1–13.

Yechieli, Y. (2000). Fresh-saline ground water interface in the western dead sea area. *Ground Water*, *38*(4), 615–623.

Yechieli, Y., Kafri, U., Goldman, M., & Voss, C. (2001). Factors controlling the configuration of the fresh-saline water interface in the dead sea coastal aquifers: Synthesis of TDEM surveys and numerical groundwater modeling. *Hydrogeology Journal*, *9*(4), 367–377.

Yechieli, Y., Shalev, E., Kiro, Y., & Kafri, U. (2010). Response of the Mediterranean and dead sea coastal aquifers to sea level variations. *Water Resources Research*, *46*. https://doi.org/10.1029/2009WR008708

Yechieli, Y., & Wood, W. (2002). Hydrogeologic processes in saline systems: Playas, Sabkhas, and saline lakes. *Earth-Science Reviews*, *58*, 343–365. https://doi.org/10.1016/S0012-8252(02)00067-3

Zhu, C., Waddell, R. K., Star, I., & Ostrander, M. (1998). Responses of ground water in the black mesa basin, northeastern Arizona, to paleoclimatic changes during the late pleistocene and holocene. *Geology*, *26*(2), 127–130.

References From the Supporting Information

AMPHOS21 (2018). *Estudio de modelos hidrogeológicos conceptuales integrados, para los salares de Atacama, Maricunga y Pedernales* (Vol. 368). Comité de Minería No Metálica CORFO.

Jordan, T. E., Mpodozis, C., Muñoz, N., Blanco, N., Pananont, P., & Gardeweg, M. (2007). Cenozoic subsurface stratigraphy and structure of the Salar de Atacama basin, northern Chile. *Journal of South American Earth Sciences*, *23*(2–3), 122–146. https://doi.org/10.1016/j.jsames.2006.09.024

Lin, Y. S., Chuang, Y. R., Shyu, J. B. H., González, G., Shen, C. C., Lo, C. H., & Liou, Y. H. (2016). Structural characteristics of an active fold-and-thrust system in the southeastern Atacama Basin, northern Chile. *Tectonophysics*, *685*, 44–59. https://doi.org/10.1016/j.tecto.2016.07.015

McCartney, J. (2001). *Hydraulic and hydrochemical interactions in the Tilopozo groundwater zone Salar de Atacama region II, Chile* (Master's thesis). National Centre for Groundwater Management, University of Technology.

Rubilar, J., Martínez, F., Arriagada, C., Becerra, J., & Bascuñán, S. (2017). Structure of the Cordillera de la Sal: A key tectonic element for the Oligocene-Neogene evolution of the Salar de Atacama basin, Central Andes, northern Chile. *Journal of South American Earth Sciences*, 1–11. https://doi.org/10.1016/j.jsames.2017.11.013